

Isotopic dependence of fusion barrier energies in reactions forming heavy elements

D. J. Hinde, M. Dasgupta, N. Herrald, R. G. Neilson,* J. O. Newton, and M. A. Lane†

Department of Nuclear Physics, Research School of Physical Sciences and Engineering, Australian National University, Canberra, ACT 0200, Australia

(Received 25 January 2007; published 7 May 2007)

The systematic dependence of fusion barrier energies on neutron excess can be determined over a broader range using radioactive nuclei. It is shown that precise measurements with a wide range of stable isotopes are necessary for optimum interpretation of radioactive beam measurements. New precision cross-section data for fusion of $^{32,34,36}\text{S}$ projectiles with Pb isotopes are presented, aiding in a revised interpretation of recent ^{38}S fusion data, which now appears more likely to follow the same trend as the stable isotopes than to show the unexpected behavior previously inferred.

DOI: [10.1103/PhysRevC.75.054603](https://doi.org/10.1103/PhysRevC.75.054603)

PACS number(s): 25.70.Jj, 25.60.Pj, 25.85.-w

I. INTRODUCTION

The formation of new, neutron-rich isotopes of heavy elements is a natural application of intense beams of radioactive neutron-rich nuclei. Because the beam intensities are inevitably lower than those of beams of stable nuclei, the practical uses of radioactive beams to form evaporation residues of the desired neutron-rich isotopes depends critically on the expected cross sections.

In such reactions, the yield of the heaviest evaporation residue peaks at beam energies close to that of the capture barrier (commonly called the fusion barrier). This is basically because of (i) increasing mass loss with increasing excitation energy due to particle evaporation and (ii) the decrease in the probability of surviving statistical fission decay with increasing excitation energy. Thus reactions with capture barriers corresponding to the lowest possible excitation energies should be most favorable. Because of the larger number of neutrons, and thus larger nuclear radius, it is expected that the energy of the capture barrier for reactions with neutron-rich isotopes of a given element will be lower than for stable isotopes. It is important to know the actual dependence of capture barrier energies on neutron number in reactions forming a given element.

There have been in recent years a number of measurements of capture excitation functions for reactions involving unstable (radioactive) neutron-rich nuclei [1–4], focusing on the dependence of the capture (fusion) barrier energy on neutron richness. The simplest expectation from an entrance-channel picture is that the fusion barrier energy should scale according to $Z_1 Z_2 / (A_1^{1/3} + A_2^{1/3})$. As a result of the larger A of a neutron-rich nucleus, this gives lowered fusion barrier energies for interactions of more neutron-rich isotopes. Barrier passing models of capture with a prescription for the calculation of the nuclear potential (for example, the Bass [5], Wilczynska-Wilczynski [6], and Sao Paulo [7] potentials) predict a

somewhat stronger dependence of capture barrier energy on neutron number. However, the recently published [4] analysis of capture cross-section measurements for the reaction of the radioactive nucleus ^{38}S with ^{208}Pb concluded that the fusion barrier was 16 ± 10 MeV lower than that for the reaction of the same target nucleus with the stable projectile ^{32}S . This difference is to be compared with model predictions, which are in the range 3 to 4 MeV, suggesting an unexpectedly large decrease in barrier energy.

If this observation were true in general, this would be a highly favorable situation for reactions using neutron-rich radioactive beams in forming neutron-rich heavy elements, as was demonstrated quantitatively in Ref. [4].

In the barrier-passing picture of capture, which involves overcoming the distribution of potential barriers in the entrance channel (resulting from channel couplings) [8,9], there is no basis for a major distinction between fusion with stable or with radioactive nuclei per se. This is because the decay of most radioactive nuclei occurs through the weak interaction, which is not expected to influence the fusion process. It is only if radioactive nuclei are so far from stability that they possess exotic collective states and/or structure (e.g., a neutron halo) that qualitatively different couplings would be expected, which could give unusual fusion behavior. Consequently, it should be possible to treat fusion of most radioactive isotopes on the same footing as fusion of stable isotopes. Thus the systematic dependence of fusion barrier energies with neutron number should not only be investigated with radioactive isotopes, but also with the widest practicable range of stable isotopes. Indeed, a combination of high-precision measurements with many stable isotopes and inevitably lower precision measurements for radioactive isotopes should give the most comprehensive picture of systematic trends. In this article, new precision measurements of capture excitation functions for reactions of stable isotopes of S and Pb are combined with the recently published cross sections discussed above for the reaction of the radioactive isotope ^{38}S with ^{208}Pb . It is demonstrated that such a combination of measurements is the most powerful approach to investigate the systematic behavior of barrier energies.

Concentrating our investigation on the properties in the entrance channel alone, we have chosen to measure capture for

*Current address: Department of Physics, Stanford University, Stanford CA94305, USA.

†Current address: Australian Public Service, Canberra, ACT, Australia.

the reactions $^{32}\text{S}+^{208}\text{Pb}$, $^{34}\text{S}+^{206}\text{Pb}$, and $^{36}\text{S}+^{204}\text{Pb}$, which all form the same compound nucleus ^{240}Cf . This nucleus decays almost exclusively by fission, thus measurement of the fission cross sections is sufficient to determine with the required accuracy the fusion (capture) cross sections. No attempt was made in this work to separate fusion-fission from a likely contribution of quasi-fission to the total fission yield. Because capture is a necessary precursor to observe either process, their sum gives the capture cross section [10].

II. EXPERIMENTAL PROCEDURE

Pulsed beams of $^{32,34,36}\text{S}$ bombarded thin enriched ($>99\%$) $^{208,206,204}\text{PbS}$ targets to form the compound nucleus ^{240}Cf . The experiments were performed over a number of separate runs, which included repeat measurements with independent normalization that gave good agreement ($\sim 1\%$) from one experiment to another.

Beams in the energy range 152–212 MeV were provided by the 14UD tandem electrostatic accelerator at the Australian National University. The beams were pulsed to allow particle identification by time-of-flight, with 1.5 ns wide beam bursts separated by 106.7 ns. The targets were of thickness 25 to $90\ \mu\text{g}/\text{cm}^2$, evaporated onto $15\ \mu\text{g}/\text{cm}^2$ C backings, which faced downstream. Target thicknesses were accurately determined by combining energy loss measurements in the monitor detectors and monitor elastic counts for fixed integrated charge.

Fission fragments were detected in the CUBE detector array [11], using two large area (284×357 mm) position sensitive multiwire proportional counters. One was located in the backward hemisphere, covering scattering angles from approximately 95° to 170° . The other was in the forward hemisphere, diagonally opposite the backward detector, covering scattering angles from 5° to 80° . Signals from the forward angle detector were only accepted if triggered by an event in the backward angle detector to minimize the data rate from elastic scattering. Where cross sections were above ~ 1 mb, fission events from the S+Pb reactions were clearly identified by energy loss and time-of-flight in the backward angle detector alone [10]. For lower yields, the kinematic coincidence requirement between the two detectors allowed background-free identification down to the lowest cross section measured (10^{-3} mb). Two Si SBD monitor detectors, placed at angles of either $\pm 15^\circ$ or $\pm 22.5^\circ$, above and below the beam axis, detected elastically scattered beam particles to allow absolute cross section normalization.

Solid angle calibration of the backward angle Multi Wire Proportional Chamber (MWPC) was achieved by simultaneous measurement of elastic scattering in the MWPC and the two monitors at a far sub-barrier energy, on a PbS or Au target. The physical detector arrangement was unchanged. At such energies, only Rutherford scattering is observed in both the monitors and the MWPC detectors. It was confirmed each time that the MWPC timing and position signals from elastically scattered sulfur exceeded the electronics timing thresholds. Using the position information from the MWPCs, and the known geometry, in the event-by-event off-line analysis the x and y position information was converted to scattering angle

θ and azimuthal angle ϕ . Placing a constant ϕ cut of 70° , and 5° wide cuts in θ in the backward-angle MWPC, the ratio of elastic counts in these cuts to the summed elastic counts in the monitors were used to determine the ratio of the solid angles of each angle cut in the MWPC to the summed solid angle of the monitors. These enabled measured ratios of fission counts to monitor elastic counts at above-barrier energies to be converted to fission differential cross sections through the known Rutherford scattering cross section in the monitors. Because the monitors were not moved between the calibration and fission measurements, accurate knowledge of their angle was not required, only that their angle was unchanged. This procedure also automatically takes into account the blocking of particles by the three 0.45 mm wires in x , and the four wires in y supporting the back detector gas window. The known folding angle of the elastic-recoil coincidences allowed checking of the geometrical calibration: agreement was within $\pm 0.1^\circ$. Absolute elastic calibrations of the detector system were carried out independently during each separate run. Repeat energies were measured in different runs, and these served to confirm the consistency of the normalization procedure (giving cross sections and anisotropies in good agreement), but were not used to normalize one run to another.

The large angular coverage of the detectors resulted in the measurement at each energy of fission angular distributions at center-of-mass angles ranging from 120° to $>170^\circ$. The angular anisotropies (discussed in Sec. IV A) and the total fission cross sections were extracted by fitting these angular distributions using the transition state model, as described in Refs. [10,11]. A subset of the angular distributions for the $^{32}\text{S}+^{208}\text{Pb}$ reaction is shown in Fig. 1. Within experimental uncertainties, the anisotropies agree with those of Ref. [12] (see also Sec. IV A). Together with the consistent quality of the fits, and the excellent agreement of repeat measurements (two angular distributions at 179.8 MeV shown in Fig. 1 almost overlap, despite being measured 4 years apart) these results give confidence in the accuracy of the measurements.

III. CAPTURE EXCITATION FUNCTIONS

The extracted fission (capture) excitation functions for the three reactions are shown on a linear scale in Fig. 2. The shape of the excitation functions are clearly very similar, and each shows a well-defined energy shift from its neighbor. This must be associated with different average capture barrier energies B_0 . To precisely determine B_0 for each reaction, the data were fitted with a barrier passing model, using the coupled-channels code CCMOD [12]. To minimize sensitivity of the deduced barrier energy to the couplings, only cross sections above 190 mb were fitted [13], corresponding to data at least 8 MeV above the average barrier energy. Test calculations with CCMOD, with no couplings and with different representative couplings included, showed a variation of the extracted B_0 of ~ 0.1 MeV, which is within statistical uncertainties. No-coupling calculations also generate only a single barrier energy, which may thus be identified to good accuracy with the desired average barrier energy. The nuclear potential used was of Woods-Saxon form, with a depth of 200 MeV for

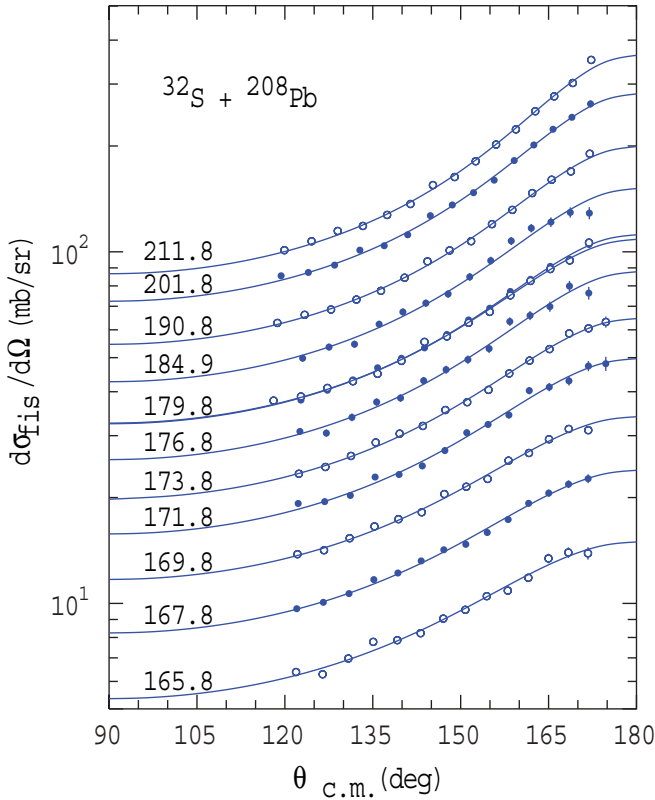


FIG. 1. (Color online) Fission angular distributions for a subset of the measurements for the $^{32}\text{S}+^{208}\text{Pb}$ reaction. The (laboratory frame) beam energy in the center of the target is indicated for each distribution. The curves show the best-fitting transition state model calculation for each energy.

all calculations. The diffuseness and radius parameters of the potential were independently varied, and the chi-squared per degree of freedom evaluated. For this, the random uncertainties on the measured cross sections were taken as the angular distribution fitting uncertainty, or 1%, whichever was larger. For each potential parameter set, the calculated barrier energy was evaluated, and the envelopes of the minimum chi-squared values as a function of potential diffuseness and barrier energy were determined. The uncertainty in the extracted parameters in this work were evaluated from the values at which the total chi-squared increases from the minimum value by the minimum chi-squared per degree of freedom or by unity, whichever was larger. The best-fitting diffuseness and barrier for each reaction were thus determined, with their associated statistical uncertainty. These are given in Table I, together with the Woods-Saxon radius parameter for the best fit.

The large nuclear potential diffuseness parameters (around 1.45 fm) required to fit the excitation functions are far from the diffuseness of ~ 0.70 fm predicted by double folding model calculations [14]. However, this discrepancy is normal, as the systematic analysis [15] of a wide range of reactions showed. Using the charge product in the entrance channel as a scaling parameter, in that work the trends of fits to nearly 50 precision fusion excitation functions were analyzed. Although there is considerable scatter in the experimental points from system to system, the trend shown in Fig. 12 (rescaled using the upper

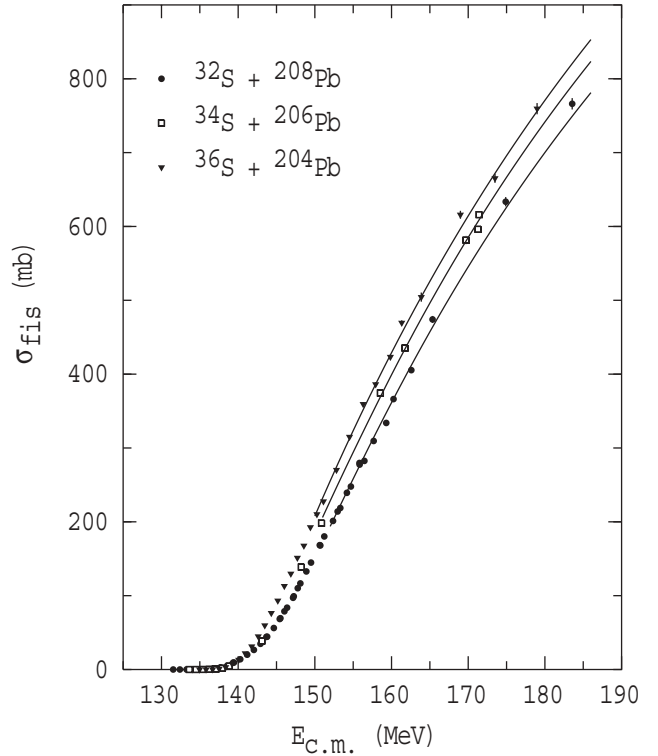


FIG. 2. Fission excitation functions for the three reactions measured in this work. The curves show the best-fitting barrier passing model fusion calculations for each reaction over the energy regions fitted.

curve of Fig. 3 in that work from 100 MeV to the current potential depth of 200 MeV) suggests a diffuseness of > 1.4 fm should be required to fit the fusion excitation functions for the present systems. Thus the excitation functions presented here are consistent with the trends of many other measurements.

In Ref. [15], it was also concluded that the diffuseness required to fit fusion excitation functions should probably be interpreted as a fitting parameter, rather than necessarily reflecting the actual nuclear potential diffuseness. This is because there may be other physical processes (such as deep-inelastic scattering), not included in barrier passing models, that can affect the fusion cross section. The consistent diffuseness values needed for the reactions measured in the present work suggest that a similar diffuseness parameter would be needed to reproduce the fusion excitation function for the $^{38}\text{S}+^{208}\text{Pb}$ reaction studied in Ref. [4]. This will be further discussed in Sec. IV C, in the reanalysis of those fusion cross sections.

TABLE I. Best-fitting barrier energy B_0 and nuclear potential diffuseness a for the reactions measured in this work, together with the radius parameter and chi-squared per degree-of-freedom for the best fit.

Reaction	B_0 (MeV)	a (fm)	r_0 (fm)	χ^2/n
$^{32}\text{S}+^{208}\text{Pb}$	144.4 ± 0.2	1.47 ± 0.04	0.911	3.3
$^{34}\text{S}+^{206}\text{Pb}$	143.1 ± 0.2	1.47 ± 0.03	0.916	1.3
$^{36}\text{S}+^{204}\text{Pb}$	142.3 ± 0.2	1.43 ± 0.03	0.926	2.3

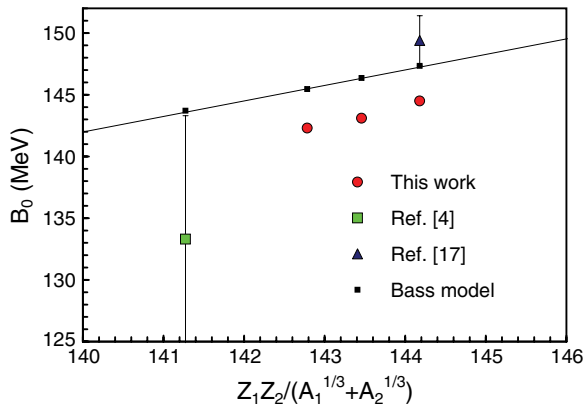


FIG. 3. (Color online) Fusion barrier energy systematics for reactions of isotopes of sulphur with lead, shown as a function of the scaling parameter $Z_1 Z_2 / (A_1^{1/3} + A_2^{1/3})$. There is a significant discrepancy between previous and current barriers for the $^{32}\text{S}+^{208}\text{Pb}$ reaction (right-most points). The line shows the trend of the calculated Bass model barriers.

IV. FUSION BARRIER ENERGY SYSTEMATICS

The extracted average fusion barrier energies for the three reaction measured here are shown in Fig. 3 by circles, plotted as a function of the scaling parameter $Z_1 Z_2 / (A_1^{1/3} + A_2^{1/3})$. The other experimental data shown are the experimental barrier energies determined in Ref. [4] for $^{32}\text{S}+^{208}\text{Pb}$ (triangle) and $^{38}\text{S}+^{208}\text{Pb}$ (square). The latter was determined by fitting new measurements for ^{38}S presented in that work, whereas the former was determined by fitting the cross sections reported in Ref [17]. For comparison, the Bass model barrier energies (with no radius shift ΔR) are indicated by the square points, and their trend by the full line.

Two key features are apparent in this comparison. The first is that the barrier energy for $^{32}\text{S}+^{208}\text{Pb}$ determined in this work, and that determined from fitting the previously measured cross sections [16,17] disagree by 5 MeV. The second is the low energy of the extracted barrier for $^{38}\text{S}+^{208}\text{Pb}$. Although it has a large assigned uncertainty, comparison of the barrier energies for these two reactions led to the conclusion [4] that the interaction barrier for $^{38}\text{S}+^{208}\text{Pb}$ is 16.1 ± 10.1 MeV lower than that for $^{32}\text{S}+^{208}\text{Pb}$. This huge and unpredicted decrease in barrier height was associated [4] with the relative neutron richness of the composite system formed. However, in view of the new results obtained in this work, that analysis needs to be revisited. The $^{32}\text{S}+^{208}\text{Pb}$ reaction will be considered first, followed by the $^{38}\text{S}+^{208}\text{Pb}$ reaction. We use a different approach to Ref. [4] to extract the barrier energy, giving a barrier energy simultaneously more accurate and more precise.

A. $^{32}\text{S}+^{208}\text{Pb}$ barrier energy

The discrepancy of 5 MeV in the extracted barrier energies from the two measurements for the $^{32}\text{S}+^{208}\text{Pb}$ reaction is statistically significant. There is a precedent for such discrepancies. Comparison of fission cross sections for the reaction $^{28}\text{Si}+^{208}\text{Pb}$ measured at ANU [10] with those measured previously [16,17] suggested that those energies

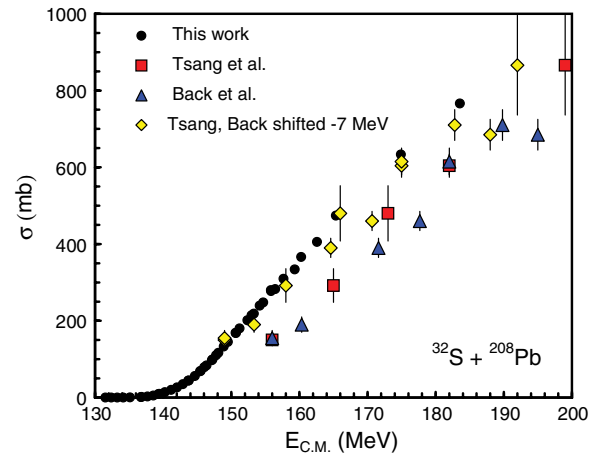


FIG. 4. (Color online) Fusion excitation functions for the $^{32}\text{S}+^{208}\text{Pb}$ reaction. The diamonds indicate the effect of shifting the data of Tsang *et al.* [16] and Back *et al.* [17] by -7 MeV, giving better agreement with the present results.

are ~ 1.5 MeV higher than the ANU energies. Although a much smaller discrepancy, it is in the same direction as that seen for the $^{32}\text{S}+^{208}\text{Pb}$ reaction. The current (filled circles) and previous (triangles and squares) cross sections for the $^{32}\text{S}+^{208}\text{Pb}$ reaction are shown in Fig. 4. There is clearly a very substantial disagreement between the two data sets. This could in principle be associated with the absolute cross-section normalization as well as a beam energy offset. The discrepancy in the barrier energies shown in Fig. 3 suggests the latter is probably the main cause. An energy shift of -7 MeV brings the lower energy cross sections of the previous data into agreement with the present data, as illustrated in Fig. 4 by the diamonds. The same energy shift also brings the two sets of fission angular anisotropies, unaffected by possible cross section normalization uncertainties, into good agreement, as illustrated in Fig. 5. However, unfortunately the energy range and the large experimental uncertainties assigned to the anisotropies of Ref. [17] do not allow a useful determination of the energy shift to be obtained from these anisotropy data.

The good energy definition and precise energy calibration [13] of the electrostatic accelerator used in this work, and the fact that the barrier energy determined [4] from the previous data [17] is higher than the Bass model prediction (which is very unusual, as noted in Ref. [4]), together suggest that the barrier energy from the present work is the more reliable. Indeed, it was already noted in Ref. [17], when discussing the $^{32}\text{S}+^{208}\text{Pb}$ results, that the fission cross sections were substantially lower than the predictions using a proximity potential model.

We discuss below features of the various methods of determining fusion barrier energies, before application to the $^{38}\text{S}+^{208}\text{Pb}$ data.

B. Fusion barrier energy determination

A number of procedures have been used to extract the average fusion barrier energy from a fusion excitation function.

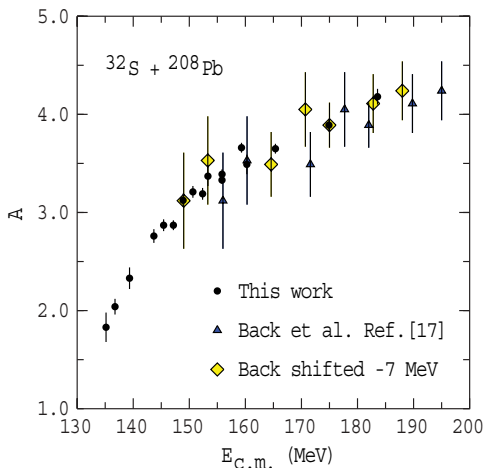


FIG. 5. (Color online) Measured fission anisotropies as a function of center-of-mass energy for the $^{32}\text{S}+^{208}\text{Pb}$ reaction. Symbols have the same meaning as in Fig. 4.

Their use depends on the available energy range and precision of the cross-section data.

1. Barrier distribution centroid

The most model-independent method to extract the mean barrier is to find the centroid of the barrier distribution [18]. This method is only possible if precision cross sections are available spanning the barrier region, from which a barrier distribution can be determined. It is appropriate if the fusion process is in competition with another process (such as incomplete fusion), and this competition may depend on the energy with respect to the barrier. This method has rarely been used, most notably for the reactions of $^{6,7}\text{Li}+^{209}\text{Bi}$ and $^9\text{Be}+^{208}\text{Pb}$, where all the above conditions applied [18]. It is unlikely to be useful in the analysis of fusion with radioactive beams in the near future, because of the requirement [8] for precise cross sections ($\sim 1\%$).

2. Above-barrier fit with a potential model

This is a very commonly used approach [13,15], in which the parameters of a Woods-Saxon nuclear potential are adjusted to give an optimum fit to above-barrier cross sections. The sum of the Coulomb and nuclear potentials then gives a single barrier, which is identified with the mean fusion (capture) barrier energy. This is the approach that was used in Sec. III to obtain the average barriers for the reactions measured in this work. To obtain an optimum fit, it is normal to vary the potential diffuseness, and either the radius or depth. The physical basis of this approach, that collisions with energies above the angular-momentum dependent barrier energy all lead to capture, has been questioned in a number of articles [15,17,19,20], particularly for collisions with a large charge product. In such cases, the diffuseness parameter required to fit the data may simply be a fitting parameter, mocking up the effects of other physical processes (such as deep-inelastic reactions) not included in the model [15]. Despite this limitation, adjusting the parameters of a Woods-

Saxon potential can reproduce very well cross sections with $\sim 1\%$ uncertainties measured over a wide energy range [11], thus is an attractive method to obtain a mean barrier energy. Including data from near-barrier energies (extending into the barrier distribution region) makes the fitting process more complicated, as then suitable couplings must be included in the calculations. Fitting cross-sections only above ~ 200 mb generally eliminates this added complexity [13]. Different codes differ in how high partial waves are handled. The code CCFULL [9] uses the incoming wave boundary condition applied at the bottom of the potential pocket inside the barrier. Clearly it requires a potential pocket for fusion to occur. In contrast, CCMOD [12] uses an analytical approximation to calculate the barrier radius and energy for nonzero angular momentum, and does not check for the presence of a pocket. Interestingly, experimental data generally show no sign of disappearance of a pocket, making CCMOD more useful in practice for determining the mean barrier. It is likely that effects of the same physical origin (friction) as those causing deep inelastic processes are also responsible for the persistence of fusion even for high partial waves.

Taking a different potential parametrization, the results of a Bass model [5] calculation for $^{32}\text{S}+^{208}\text{Pb}$ are shown in Fig. 6. Despite matching the barrier energy by a radius shift ($\Delta R = 0.25$ fm), the slope of the calculation is much steeper than that of the data. Fitting the data with this model would lead to an erroneous barrier energy, as the slope does not match that of the measured excitation function.

The difference in slope may be caused in part by competition from deep-inelastic reactions, having large energy loss. This was already suggested in Ref. [17] to explain the big difference between their measured fission cross sections and proximity model calculations of fusion. As seen by comparing

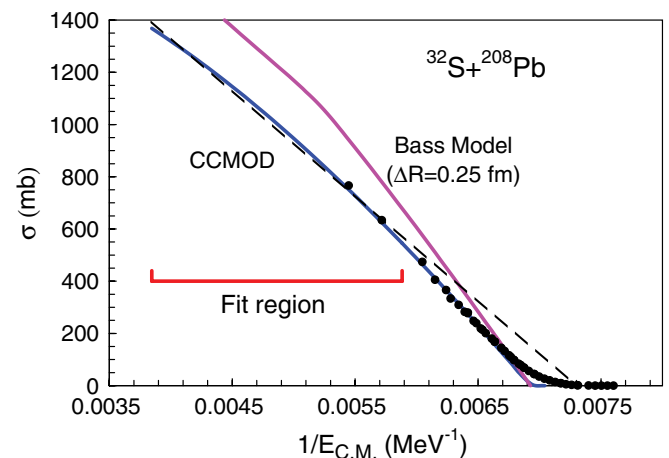


FIG. 6. (Color online) Measured and calculated (no coupling) CCMOD fusion cross sections as a function of $1/E_{c.m.}$ for the $^{32}\text{S}+^{208}\text{Pb}$ reaction. The dashed line shows the linear fit to the region of the calculated excitation function whose energy range is indicated by the horizontal line, corresponding to a lower cutoff energy of 170 MeV. The intercept with the x axis indicates a barrier energy much lower than the actual energy. A Bass model calculation having the same barrier energy is also shown, predicting substantially larger cross sections than measured.

Figs. 4 and 6, for the present data, the fraction of deep-inelastic events would be much less than postulated to explain the earlier data [17].

In summary, fitting measured fusion excitation functions with a potential model can give a very good reproduction of the data. However, without a parameter in the model to scale the cross sections independently of the barrier energy, determining the barrier energy through fitting cross sections can easily lead to error. For a Woods-Saxon potential, the *effective* diffuseness parameter (determining the barrier radius in the model) is the variable that allows the slope of the excitation function to be fitted. The linear fit method as described below has this freedom but also has significant limitations, as detailed below.

3. Linear fit vs. $1/E_{c.m.}$

This method was used in Ref. [4] to extract the barrier energy for the $^{38}\text{S}+^{208}\text{Pb}$ reaction. It is based on the approximate expression for the fusion cross-section σ as a function of energy $E_{c.m.}$: $\sigma = \pi R_0^2(1 - E_{c.m.}/B_0)$. The approximation lies in the replacement of the true energy-dependent (angular momentum dependent) barrier radius by a fixed barrier radius R_0 . This approach does not require any parametrization of the nuclear potential, though use of a square-well nuclear potential would result in a fixed barrier radius. In the fitting process there is no link between B_0 and R_0 through a nuclear potential. Thus it could be argued that this approach is model independent. However, it is demonstrated below that the implicit assumption of a fixed R_0 can lead to substantial errors in the extracted average barrier energies.

This is investigated by applying this fitting method to simulated experimental cross sections for the reaction $^{32}\text{S}+^{208}\text{Pb}$ calculated with the code CCMOD. These included no couplings, so that there is a single well-defined barrier energy and radius. The nuclear potential parameters were those that matched the experimental above-barrier cross sections. The data (circles) and calculation (curve labeled CCMOD) are shown in Fig. 6. A subset of the calculated cross sections spanning an energy range from a variable lower energy cutoff to the maximum calculated energy of 260 MeV were fitted using the linear fit method. For the case shown in Fig. 6, the cross sections fitted correspond to the bracketed energy region labeled “fit region,” having a lower cutoff energy (E_{cutoff}) of 170 MeV. The best-fitting straight line to this region is shown by the dashed line. It clearly gives an extrapolated barrier energy well below the actual barrier. The closer the fitting cutoff is to the actual barrier, the smaller is the deviation. This is illustrated in Fig. 7, where the barrier energy (B) determined from the linear extrapolation divided by the actual barrier (B_0) is plotted as a function of the ratio of E_{cutoff} to B_0 . The size of the discrepancy depends on how far the fitted data extend toward the barrier. If the data extended down to 5% above the barrier energy, in this case the error is less than 1%. The magnitude of the discrepancy also depends on the deviation of the experimental cross sections from a linear form in the $1/E_{c.m.}$ representation. If the nuclear diffuseness needed to reproduce the excitation function were smaller, the discrepancy would be smaller.

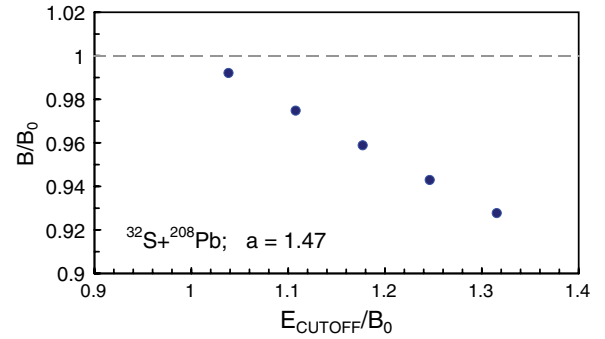


FIG. 7. (Color online) Results from the fitting process illustrated in Fig. 6, where ratios of the extrapolated barrier energies B to the actual energy B_0 , are shown as a function of the ratio of the low energy cutoff in the fit to B_0 . Naturally, the closer the fitted region is to the barrier energy, the smaller is the discrepancy in B .

C. $^{38}\text{S}+^{208}\text{Pb}$ barrier energy

The eight experimental cross sections reported for $^{38}\text{S}+^{208}\text{Pb}$ include two data points that the authors [4] rejected on the basis that they were outliers compared with the trend of the remaining six points. The data are shown in Fig. 8 by circles, with the rejected data points indicated by open circles. In Ref. [4] the linear fit in a $1/E_{c.m.}$ representation produced a barrier energy of 133.3 ± 10.0 MeV. Using the fitting code DESCALC, we obtain 134.0 ± 6.2 MeV, with a chi-squared per point of 0.21. These barriers are in satisfactory agreement, though our uncertainty is somewhat smaller. As expected, fitting the full data set (including the open circles) gives a considerably lower barrier energy, of 126.3 ± 5.2 MeV, with a chi-squared per point of 1.40. These results, and others

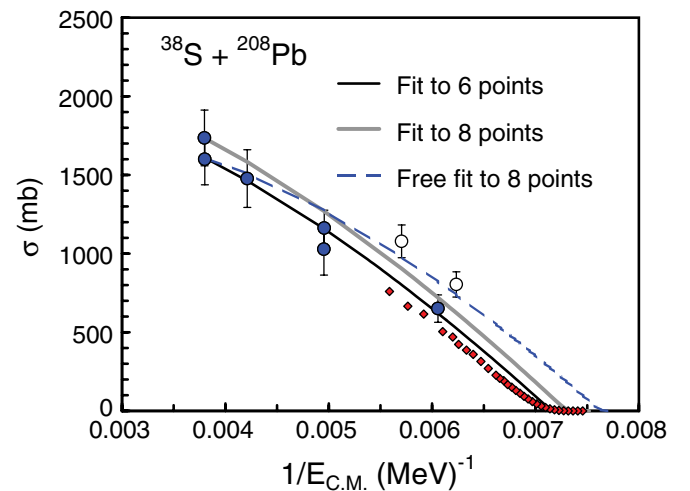


FIG. 8. (Color online) Measured fusion cross sections as a function of $1/E_{c.m.}$ for the $^{38}\text{S}+^{208}\text{Pb}$ reaction (circles). The outlined circles indicate the data points rejected in Ref. [4] as being outliers. The full black curve shows the fit to the filled circles, whilst the grey curve shows the fit to all 8 data points, both calculations having the nuclear potential diffuseness fixed at 1.43 fm. The dashed curve shows the unconstrained fit to all eight data points. The small diamonds show for reference the current data for the $^{36}\text{S}+^{204}\text{Pb}$ reaction, from which the diffuseness value of 1.43 fm was determined.

TABLE II. Best-fitting barrier energies B_0 and nuclear potential diffuseness a to all 8 and to the 6 acceptable cross sections for the $^{38}\text{S}+^{208}\text{Pb}$ reaction. The chi-squared per degree-of-freedom is also given.

Method		8 data points	6 data points
Ref. [4]	B_0 (MeV)		133.3 ± 10.0
$1/E_{c.m.}$ fit	B_0 (MeV)	126.3 ± 5.2	134.0 ± 6.2
	χ^2/n	1.40	0.21
a varied	B_0 (MeV)	132.0 ± 2.9	139.3 ± 4.5
	a (fm)	1.80 ± 0.20	1.40 ± 0.30
	χ^2/n	1.08	0.21
$a = 1.43$	B_0 (MeV)	136.8 ± 1.1	139.5 ± 1.6
	χ^2/n	1.57	0.21

obtained below, are presented in Table II. The lowest measured cross section in this data set is $\sim 20\%$ above the barrier, thus the results of Fig. 7 suggest that these barrier energies may be $\sim 5\%$ too low.

In view of this likely error, the $^{38}\text{S}+^{208}\text{Pb}$ cross sections are here fitted using the potential barrier-passing model, in the same way as the data for the stable isotopes (the nuclear potential diffuseness and radius parameter were independently varied, maintaining a constant potential depth of 200 MeV). As expected, the barrier energies (see Table II) determined by this method are higher, by ~ 5 MeV. Fitting only the 6 data points, the best-fitting diffuseness parameter is 1.40 ± 0.30 fm, in good agreement with the values of 1.43 – 1.47 required to fit the fusion data for the stable sulfur isotopes. The fit to all 8 data points, as indicated by the dashed line in Fig. 8, required a diffuseness of 1.80 ± 0.20 . This large value of the diffuseness can be taken as supporting the rejection of the two outlying cross-sections – despite the chi-squared per degree-of-freedom (1.08) being quite acceptable. Using the six acceptable ^{38}S data points, the extracted barrier energy of 139.3 ± 4.5 MeV is the most precise that can be obtained, without making use of the stable isotope results, in the procedure described below.

The fitted diffuseness parameter of 1.40 fm (despite its uncertainty) may be taken as experimental support for the contention that the potential diffuseness required to fit the ^{38}S data should not be different from those determined more precisely for the stable isotopes. Then in the fitting, the diffuseness can be fixed, which will result in a barrier energy with smaller uncertainty. Using $a = 1.43$ fm (the value required for ^{36}S), the best-fitting barrier energies are 136.8 ± 1.1 MeV for all 8 data points, and 139.5 ± 1.6 MeV for the 6 data points. Figure 8 shows the fixed diffuseness fits to all data (full gray curve) and to the 6 data points (full black curve). Also shown are the present data for $^{36}\text{S}+^{204}\text{Pb}$ from which the fixed diffuseness parameter used was determined.

The barrier energy systematics presented in Fig. 3 must now be revised, based on the new analysis presented above. These new barrier energies are shown in Fig. 9 on an expanded energy scale. The dashed line shows the empirical trend established by the new data for the reactions with the stable isotopes $^{32,34,36}\text{S}$. It is in good agreement with the barrier energy of 139.5 ± 1.6 MeV determined from the six data points for ^{38}S , taking

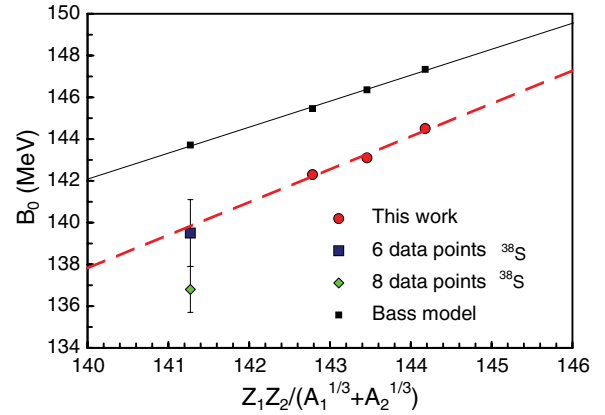


FIG. 9. (Color online) As Fig. 3, with an expanded energy scale. The barriers for the $^{38}\text{S}+^{208}\text{Pb}$ reaction (left-most points) are derived from the new analysis using the potential model fit with fixed diffuseness $a = 1.43$ fm, as discussed in the text.

$a = 1.43$ fm. This suggests no unusual behavior for fusion with the radioactive ^{38}S isotope.

The above conclusion relies on the two outlier cross sections for ^{38}S being rejected. As demonstrated, if they are included in the fit, and the diffuseness is not constrained to be the same as for the stable isotopes, a barrier energy of 132.0 ± 2.9 MeV results—a value far from that expected. The interpretation depends critically on the uncertainties assigned to the ^{38}S cross sections. If the random uncertainties would be substantially smaller than the quoted error bars, this fit would give an unacceptable χ^2/n , rather than 1.08, and the outliers would then definitely have to be rejected. If the error bars truly reflect the random scatter expected, the fact that this unconstrained potential model fit to all the data gives an acceptable χ^2/n of 1.08 weakens the case to reject the two outlier points. It is concluded that for this reason, there must still be some doubt about whether the measured capture barrier energy for the $^{38}\text{S}+^{208}\text{Pb}$ reaction is consistent with the trends now well-determined for the stable S isotopes. However, equally, it is now difficult to conclude that the barrier energy in this reaction is definitely anomalously low. If we accept the elimination of the two outlier points, as proposed by those who made the measurements [4], then the most likely barrier energy for the $^{38}\text{S}+^{208}\text{Pb}$ reaction is 139.5 ± 1.6 MeV.

V. SUMMARY AND CONCLUSIONS

Lower beam intensities of radioactive nuclei compared with stable isotopes make it more difficult to determine the key characteristics of the fusion process. The most basic characteristic of fusion is the energy of the average barrier. It has been demonstrated here that the method of linear fitting of the cross sections plotted as a function of $1/E_{c.m.}$ can lead to significant underestimation of the average barrier, and should not be used unless cross section measurements extend down to 5% above the barrier. Instead, the use of a potential barrier passing model (such as implemented in the code CCMOD) can be a better approach.

In fitting the recently published [4] fusion cross sections for $^{38}\text{S}+^{208}\text{Pb}$, the latter method leads to a barrier energy higher

by 5 MeV than the former. Fitting the new precision measurements of the fusion excitation function for the $^{32}\text{S}+^{208}\text{Pb}$ reaction showed that the barrier energy is 144.4 MeV, rather than 149 MeV, as the fit of Ref. [4] to the previous data of Ref. [17] indicated. In combination, these two new barrier energies, contributing almost equally, change the difference in barrier energies found in the reactions of ^{208}Pb with ^{32}S and ^{38}S from 16 ± 10 MeV to 4.9 ± 1.6 MeV. This is not inconsistent with the Bass model, which predicts an energy difference of 3.6 MeV.

A major factor in reducing the uncertainty in the experimental barrier energy for the reaction with the radioactive ^{38}S was the use of the *effective* diffuseness of the nuclear potential obtained by fitting the fusion excitation functions of the stable isotopes $^{32,34,36}\text{S}$, reported in this work. This allowed the

fitting parameter space to be significantly restricted, leading to determination of the barrier energy with 3–6 times smaller uncertainty. This is a very attractive advantage for radioactive beam measurements where high statistics (small uncertainties) are very difficult to achieve. Thus, the precision measurement of fusion excitation functions for reactions of neighboring stable isotopes should be a key component of future fusion investigations with radioactive beams.

ACKNOWLEDGMENTS

D.J.H. and M.D. acknowledge the financial support of an Australian Research Council Discovery Grant. The authors are grateful to R. D. Butt, A. C. Berriman, C. R. Morton, H. Timmers, and R.A. Yanez for assistance in running the experiments at various times.

-
- [1] K. E. Zyromski *et al.*, Phys. Rev. C **63**, 024615 (2001).
 - [2] Y. Watanabe *et al.*, Eur. Phys. J. A **10**, 373 (2001).
 - [3] J. F. Liang *et al.*, Phys. Rev. Lett. **91**, 152701 (2003); **96**, 029903(E) (2006).
 - [4] W. Loveland *et al.*, Phys. Rev. C **74**, 044607 (2006).
 - [5] R. Bass, Phys. Rev. Lett. **39**, 265 (1977).
 - [6] K. Siwek-Wilczyńska and J. Wilczyński, Phys. Rev. C **69**, 024611 (2004).
 - [7] L. R. Gasques *et al.*, Nucl. Phys. **A764**, 135 (2006).
 - [8] M. Dasgupta, D. J. Hinde, N. Rowley, and A. M. Stefanini, Annu. Rev. Nucl. Part. Sci. **48**, 401 (1998).
 - [9] K. Hagino, N. Rowley, and A. T. Kruppa, Comput. Phys. Commun. **123**, 143 (1999).
 - [10] D. J. Hinde *et al.*, Nucl. Phys. **A592**, 271 (1995).
 - [11] D. J. Hinde A. C. Berriman, M. Dasgupta, J. R. Leigh, J. C. Mein, C. R. Morton, and J. O. Newton, Phys. Rev. C **60**, 054602 (1999).
 - [12] M. Dasgupta *et al.*, Nucl. Phys. **A592**, 271 (1995).
 - [13] J. R. Leigh *et al.*, Phys. Rev. C **52**, 3151 (1995).
 - [14] I. I. Gontchar, D. J. Hinde, M. Dasgupta, and J. O. Newton, Phys. Rev. C **69**, 024610 (2004).
 - [15] J. O. Newton *et al.*, Phys. Lett. **B586**, 219 (2004); J. O. Newton, R. D. Butt, M. Dasgupta, D. J. Hinde, I. I. Gontchar, C. R. Morton, and K. Hagino, Phys. Rev. C **70**, 024605 (2004).
 - [16] M. B. Tsang *et al.*, Phys. Rev. C **28**, 747 (1983).
 - [17] B. B. Back *et al.*, Phys. Rev. C **32**, 195 (1985); **33**, 385(E) (1986).
 - [18] M. Dasgupta *et al.*, Phys. Rev. C **70**, 024606 (2004).
 - [19] F. L. H. Wolfs, Phys. Rev. C **36**, 1379 (1987).
 - [20] J. G. Keller *et al.*, Phys. Rev. C **36**, 1364 (1987).